Preprint
UCRL-JC-146506

Microbiologically-Facilitated Effects on the Surface Composition of Alloy 22, A Candidate Nuclear Waste Packaging Material

J.M. Horn, T. Lian, S.I. Martin

This article was submitted to
NACE International Corrosion 2002, Denver, CO, April 7-12, 2002

December 7, 2001

MICROBIOLOGICALLY-FACILITATED EFFECTS ON THE SURFACE COMPOSITION OF ALLOY 22, A CANDIDATE NUCLEAR WASTE PACKAGING MATERIAL

Joanne Horn
Tiangan Lian
Sue Martin
Lawrence Livermore National Laboratory
7000 East Ave.
Livermore, CA 94550

ABSTRACT

The effects of microbiological activities on the surface composition of Alloy 22 was investigated. Prior studies suggesting microbially-generated selective dissolution of chromium from Alloy 22 were based solely on analyzing solubilized Alloy 22 elements. These and other investigations point to the insufficiencies of analyzing solubilized (or solubilized and re-precipitated) alloying elements to discern between homogeneous/stoichiometric dissolution and selective/non-stoichiometric dissolution of alloying elements. Therefore, an approach using X-ray Photoelectron Spectroscopy (XPS) to interrogate the surface layers of treated Alloy 22 specimens was taken to resolve this issue. Sputtering into the surface of the samples, coupled with XPS analysis at given intervals, allowed a high resolution quantitative elemental evaluation of the alloy as a function of depth. Biotically-incubated Alloy 22 show a region that could be depleted of chromium. Surfacial XPS analysis of these same coupons did not detect the presence of re-precipitated Alloy 22 component elements, also supporting the possible occurrence of non-stoichiometric dissolution. Thus, these preliminary data do not exclude the possibility of selective dissolution. It also appears that this experimental approach shows promise to unequivocally resolve this issue. Further tests using smoother-surface, more highly polished coupons should allow for better resolution between surface layers to permit a decisive determination of the mode of Alloy 22 dissolution using sputtering XPS analysis.

Key words: MIC, Yucca Mountain, Alloy 22, nuclear waste, passive corrosion, dealloying

INTRODUCTION

Highly corrosion resistant materials are required for containment of high level nuclear wastes, which must remain safely isolated for thousands of years. The current design of waste packages for a prospective nuclear waste repository at Yucca Mountain, Nevada (YM) include an inner structural support of Type 316 nuclear grade stainless steel surrounded by an outer 2 cm barrier of Alloy 22 (UNS N06022; Table 1) to provide corrosion resistance. Passive dissolution rates of Alloy 22 have been estimated to be on the order of 0.05-0.5 μm/yr[1,2], which would provide for a sufficient period of waste containment. Localized corrosion of Alloy 22 is largely prevented by the presence of a passive film composed of nickel and chromium oxides[3]. Therefore, selective dissolution of elements within the protective oxide layers would result in susceptibility to localized corrosion. Localized corrosion might occur as solubilized elements were replaced by migration from the base metal, if the oxide film was solubilized completely when dissolution rates exceed replacement through migration, or if spalling of the oxide film occurred due to accumulation of voids at the base metal-film interface[4].

Endpoint chemical analyses of bulk aqueous fractions from linear polarization studies of bacterially-inoculated and sterile Alloy 22 coupons incubated for four to five months showed evidence of biotically-induced processes that may contribute to surface elemental dissolution of Alloy 22. Soluble chromium concentrations on the order of 1 ppm were found in the aqueous media after incubation of Alloy 22 with YM bacteria, while no solubilized chromium was detected in parallel sterile controls[5] (Table 3). Dunn and coworkers also demonstrated chromium and molybdenum dissolution from Alloy 22 in potentiostatic polarization tests under a variety of abiotic conditions[1]. Generalized corrosion with stoichiometric dissolution of all elements (i.e., dissolution of all metal elements at the same rates) could have occurred in either of these experiments, followed by selective precipitation of some elements (Fig. 2). Assessing endpoint elemental concentrations in solution can not account for the possible precipitation of previously solubilized elements indicative of a homogeneous mode of dissolution. In this regard, Dunn et al. found some redeposition of nickel, chromium, and molybdenum on the platinum counter electrode and precipitates on test specimens[1]. A mass balance of solubilized and reprecipitated components in such systems though, is very difficult to perform in order to unequivocally distinguish between selective or generalized dissolution of Alloy 22. In an effort to better define these processes, and determine the potential microbiological contribution to them, the surfaces of Alloy 22 test samples which had undergone linear polarization analysis while colonized by YM bacteria were interrogated using sputtering X-Ray Photoelectron Spectroscopy (XPS), and compared to parallel sterile control and unexposed Alloy 22 samples. The approach taken to determine whether homogeneous or selective dissolution had occurred was thus to assess the relative amounts of the major elements composing Alloy 22 as a function of depth into the sample, rather than trying to account for the amounts of solubilized and precipitated elements.

Table 1. Composition of Alloy 22*

C (%)	Mn (%)	S (%)	Co (%)	Mo (%)	Si (%)	Cr (%)	W (%)	V (%)	Fe (%)	P (%)	Ni (%)
0.002	0.260	0.001	0.510	13.40	0.025	21.58	2.820	0.150	3.95	0.012	Bal. (57.29)

* weight percent

EXPERIMENTAL METHODS

Experimental Conditions and Alloy 22 Sample Preparation

Figure 1 depicts a schematic diagram of the corrosion cell designed to allow the interaction between test specimens, the test medium, and introduced microorganisms, as well as facilitate implementation of DC linear polarization technique. A cylindrical glass flange with O-ring seals was clamped to a working electrode sheet specimen, which formed the bottom of the vessel. The corrosion cell allowed a total of 28.3 cm^2 of exposed area on the coupon specimen (or working electrode). A platinum wire was used as an auxiliary electrode, while a commercial saturated calomel electrode (SCE) was used as reference electrode.

Alloy 22 (UNS N06022; Table 1) specimens were received as flat circular disk coupons (2.75 in.; 7 cm diameter). The exposed side of coupons were wet-polished with abrasive paper progressively to 600-grit, cleaned with acetone and distilled water, and assembled cells were then sterilized by autoclaving.

Twelve strains of YM bacteria, including acid, slime, and sulfide producers, as well as iron-oxidizing bacteria (Table 2) were mixed and applied to coupon surfaces. Microbial cell densities were established before aseptically combining and spreading a defined number (at least 10^8 bacterial cells of each strain) of all isolates on specimens which were air dried before they were exposed to growth media in corrosion cells. The growth medium was composed of R2 bacterial medium (450 ml/corrosion cell), a low-nutrient formulation[6], supplemented with 0.5% glucose and 0.75% protease peptone #3 (Difco, Detroit, MI) in 100X simulated J-13 well water (water from the vicinity of YM[7] site). Simulated 10X J13 well water was composed of 153 mM $NaHCO_3$, 8.6 mM Na_2SO_4, 7.6 mM NaF, 96 µM Na_2SiO_3, 8.7 mM $MgSO_4$, 5.2 mM $CaCl_2$, 37 mM $CaCO_3$, 5.2 mM $Ca(NO_3)_2$, 90 µM H_2SO_4, 10 µM HCl, 8.6 mM KCl, 10 µM $KHCO_3$. All vessels were incubated at room temperature (approximately 22°C) for a period of four to five months. To determine the microbial effects on corrosion behavior, an identical set of corrosion cells, which did not contain bacteria and were maintained in a sterile condition, were constructed. Linear polarization data resulting from these experiments has been reported previously[5].

Following the four to five month incubation period, test cells were dissembled and coupons were dried and stored under nitrogen, then fixed in 2% glutaraldehyde for Scanning Electron Microscopy/Energy Dispersive Spectral Analysis (SEM/EDS) and subsequent XPS.

Analytical Techniques

Aqueous fractions. Samples of spent media were collected at the termination of the incubation period (4-5 months), after all polarization data had been collected, and each was acidified to pH 2 with HCl to maintain the solubility of contained ions before being analyzed by Inductively Coupled Plasma Atomic Emission Spectrometry (ICP-AES; Applied Research Laboratories, Model 3560 equipped with a simultaneous optical system, Rowland Circle) was employed to determine the concentrations of metals relevant to Alloy 22 coupon composition (Table 3). These elements were also analyzed in solution samples collected from sterile control systems to ascertain the concentration of metal components contributed by abiotic corrosion processes. Parameters of analysis were: incident power, 1150KW; net gas flow rate, 0.4 L/min; plasma gas flow rate, 16 L/min; reflected power, <2 KW.

SEM/EDS. Following glutaraldehyde fixation, all coupons were imaged and analyzed using SEM/EDS (Hitachi, Model S-800) at an accelerating voltage of 25 kV, with a magnification of 1000X for EDS and elemental dot mapping using a Be window.

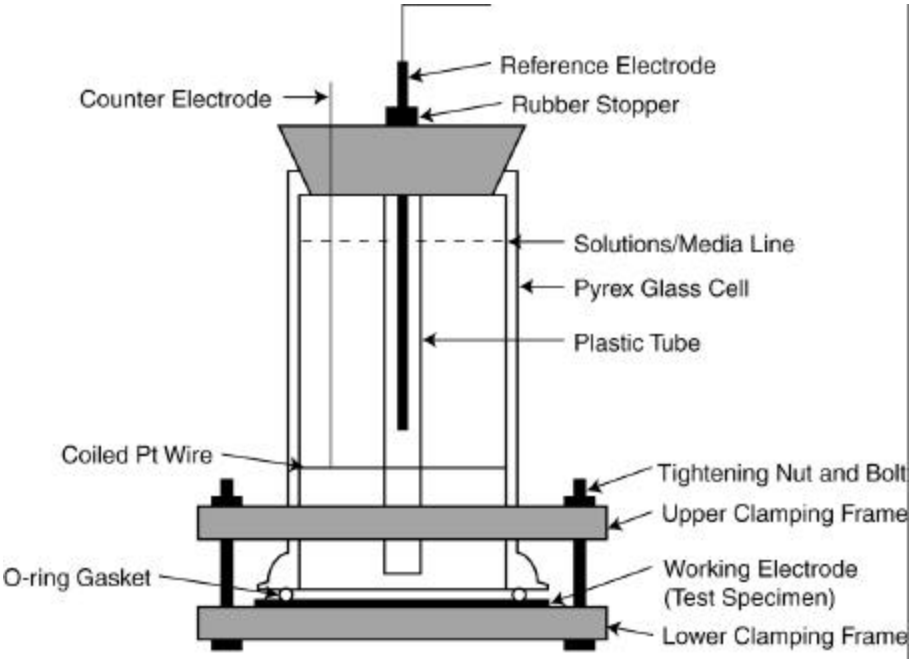

Figure 1. Configeration of experimental vessels used for electrochemical and dissolution experiments.

XPS. XPS experiments were performed on a Physical Electronics 5400 ESCA system using 15 kV Mg Kα radiation (1253.6 eV) or Al Kα radiation (1486.6 eV) and a spherical capacitor analyzer with a pass energy of 17.90 eV giving an overall energy resolution of 1.0 eV. All binding energies are referenced to the Fermi level of the analytical instrument as calibrated to the Au 4f peaks. Binding energies were further referenced to the C 1s photoelectron line arising from adventitious carbon at 284.6 eV to account for charging effects.

RESULTS and DISCUSSION

ICP

After five months incubation, at the termination of linear polarization studies, aqueous media from both bacterially-inoculated and sterile corrosion vessels were sampled and subjected to ICP analysis to determine the concentrations of solubilized Alloy 22 components. Fresh medium, which had never been exposed to corrosion vessels, was likewise assessed for comparison. Results showed chromium concentrations (approximately 1 ppm) in test vessels that had been inoculated and

Table 2. List of YM Bacteria Inoculated on Alloy 22 Coupons

LLNL Strain #	Species Identification	Characterization
ESF-71h-RT-4	*Flavobacterium esteroaaromaticum*	Acid producer
ESF-71h-RT-4	*Flavobacterium*	Acid producer
ESF-C1	*Cellulomonas flavigena*	Acid producer
LB-71h-50-3	*Bacillus*	Acid producer
LBan-U7	Unidentified	Acid producer
LB-C1	Unidentified	Slime producer
LB-71h-50-4	*Bacillus subtilus*	Slime producer
LB-71h-50-6	*Bacillus sp.*	Slime producer
LB-71h-RT-15	*Pseudomonas pseudoflava*	Slime producer
LBan-U3	*Bacillus pantothentics*	Slime producer
68	Unidentified	Iron oxidizer
69	Unidentified	Iron oxidizer
	Sulfate Reducing Bacteria	Sulfide producer

incubated with YM bacteria, but no chromium was detected in sterile vessels incubated for the same period, or in unexposed media (Table 3). Additionally, a lower concentration of nickel (0.1 ppm) was found solubilized in vessels incubated with YM bacteria, but none was detected in media from sterile control experiments, or in fresh media. Iron was detected in all media tested. The presence of solubilized chromium (and nickel) in vessels incubated under biotic conditions suggested that the applied YM bacteria might be causing a surface dissolution from Alloy 22. Thus, further assessment was undertaken to evaluate the surface chemistry of test coupons.

Table 3. Dissolution of Alloy 22 Elements in Aqueous Medium After 5-Month Exposure to YM Bacteria

Vessel conditions/Material	Fe (mg/l)	Cr (mg/l)	Ni (mg/l)	Mo (mg/l)
Unexposed, fresh medium	0.25	n.d.*	n.d.	n.d.
Alloy 22 Sterile, no bacteria	0.42	n.d.	n.d.	n.d.
Alloy 22 + YM Bacteria	0.32	1.05	0.1	n.d.

* not detectable

SEM/EDX

SEM images at 1,000-10,000X magnification showed particulates on the surfaces of coupons; these were very numerous on the bacterially-inoculated coupons (data not shown). The corrosion cell design that was used for these experiments had the working electrode/Alloy 22 sample emplaced at the base of the cell, forming the floor of the apparatus (Fig. 1). Therefore, if homogeneous corrosion was occurring and some of the elements had reprecipitated, then it was likely that at least some of this material might be deposited on the Alloy 22 sample. Therefore EDS analysis was used to determine the elemental composition of detected precipitates on coupon surfaces. EDS analyses in spot mode showed that one particulate on a nonsterile coupon was chromium rich, although most were silica-enriched. The observed silicon precipitated from the 100X J13 fraction of the growth media, while the chromium was most probably a result of the reduction of solubilized Cr(VI) to insoluble Cr(III). EDS dot maps

of six separate areas each on inoculated and unexposed coupons, however, did not show any significant differences in elemental compositions between any of the inspected regions (data not shown). Further, no definitive differences in surface morphology could be discerned.

XPS

The depth of penetration of x-rays used for EDS analysis on the surface of the studied coupons may be as great as 1 µm. It was therefore possible that impinging x-rays could penetrate as far as unaffected base metal, accounting for the lack of elemental difference that was evident using EDS dot mapping between differently treated samples. Therefore, higher-resolution sputter XPS analysis was used to evaluate the surface layers of coupons to determine elemental compositions on an inoculated coupon, and one incubated under sterile

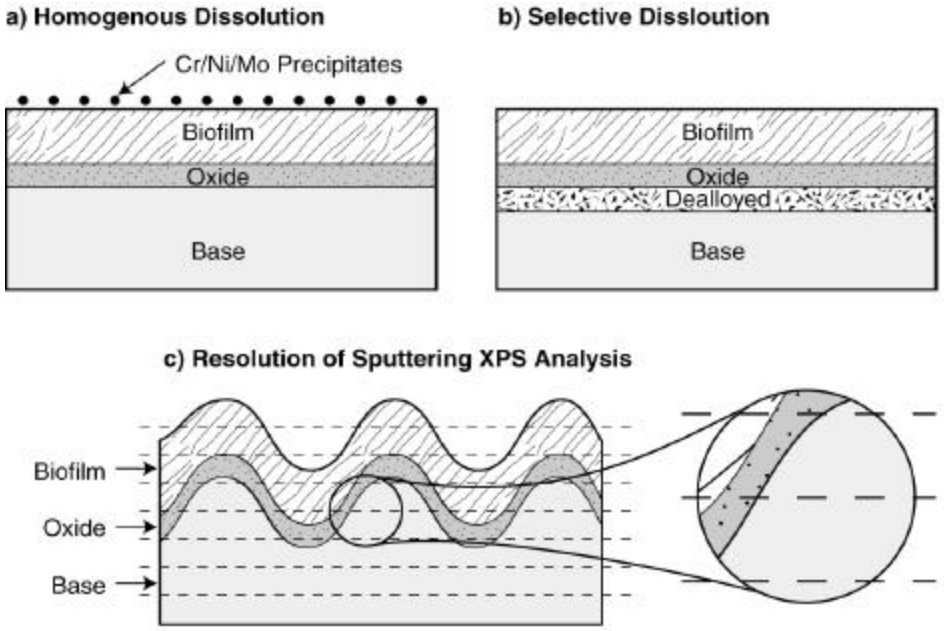

Figure 2a - 2c. Configuration of potential layers of materials on biotically-incubated Alloy 22 coupons. Panel a) Extant layered material if generalized, stoichiometric dissolution of Alloy 22 is occurring; note that even if only select alloying elements are found solubilized, others could exist as precipitates on the surface of the coupon. Panel b) Extant layered material if selective dissolution of Alloy 22 is occurring. The aim of sputtering XPS analysis is to distinguish between the scenario depicted in Panel (a) versus Panel (b). Panel c) The roughness of the Alloy 22 coupons (600 grit) and associated layers of material. XPS analysis (1 mm) covers a greater area than the scale of roughness of the Alloy 22 coupons. Therefore, for any given depth of analysis, more than a single layer of material can be sampled, producing a loss of resolution in analytical results between the layers.

conditions. Sputtering into the surface of sterile, inoculated, and unexposed coupons at a rate of 20 angstroms/min with XPS analysis of sputtered material at pre-determined intervals showed marked differences between sterile, inoculated, and unexposed coupons.

The inoculated coupon had a thick layer of carbonaceous material which asymptotically fell to low levels after sputtering approximately 4000 angstroms into the surface. The sterile control coupon, in contrast, had a thin layer of surface carbon that decreased to less than 10% of the total elemental composition within 300 angstroms of the surface (Fig. 3). Therefore, at any given depth of analysis, differently treated coupons could not be compared; clearly the

inoculated surface of Alloy 22 after five months of incubation had an extensive biofilm coating that wasn't present on the sterile control. Furthermore, because the surfaces of these coupons were polished to 600 grit they are relatively rough, while the area of analysis is comparatively large, on the order of a mm^2. Therefore, at any given depth of analysis more than a single layer of material could be analyzed (Fig. 2), producing poor definition of any defined layers that may be present. Despite these caveats, a biofilm could be identified on the inoculated coupon even though its defined depth limit may be somewhat uncertain.

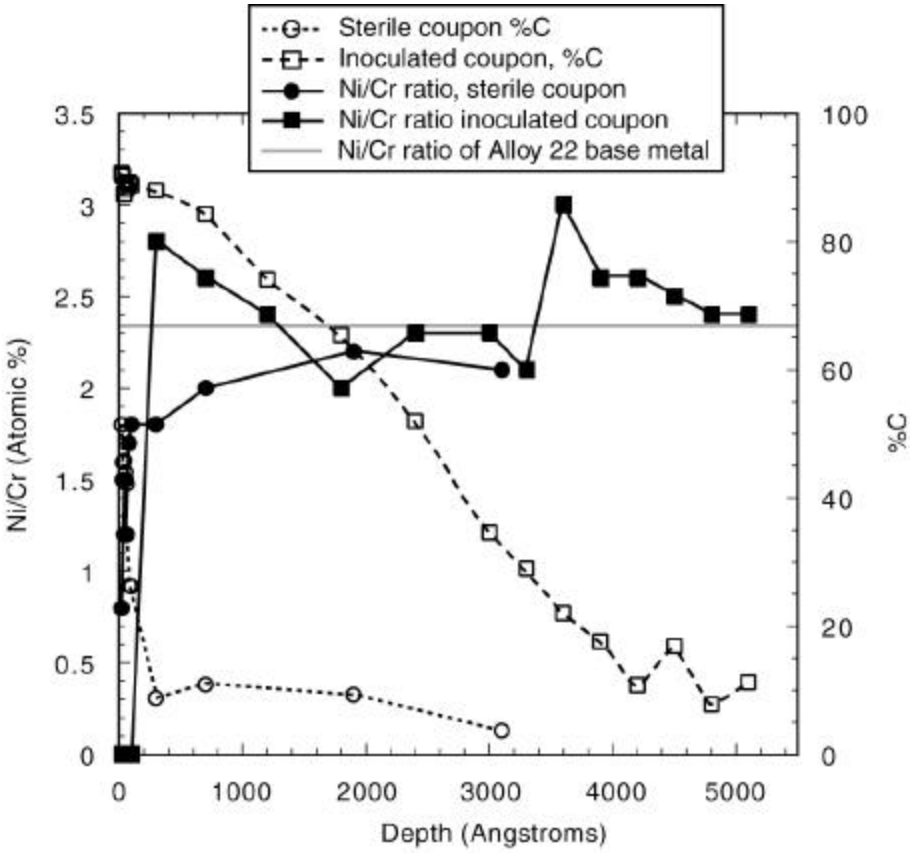

Figure 3. Nickel to chromium ratio and percent carbon as a function of depth in inoculated and sterile Alloy 22 coupons. For each point, the inherent analytical margin of error is +/– 0.5 atomic %.

Solubilized chromium was found in the medium in which the bacterially-inoculated coupon had incubated (Table 3), therefore ratios of Ni:Cr were used as a means of evaluating the extent of selective dissolution, if any, on this sample. The Ni:Cr atomic ratio on the Alloy 22 incubated under sterile conditions became constant at values of 1.8-2.2 within an analytical depth of 80-100 angstroms, the same relative depth where carbon content had fallen to low levels (Fig. 3). Presumably, this indicated that any organic deposition generated from the medium and the protective oxide layer had been traversed and that the consistent Ni:Cr ratio with increasing depth into the metal surface was indicative of the base metal composition.

The nonsterile incubated coupon showed somewhat different Ni:Cr ratios. Commensurate with the lowest carbon levels (showing that the biofilm had been traversed), Ni:Cr ratios remained between 2.4-3.0; Ni:Cr ratios actually decreased steadily from 3.0 at a depth of 3600 angstroms to 2.4 at 5100 angstroms. These elevated levels of nickel (in comparison with the sterile-incubated base metal value of 1.8-2.2) may be indicative of a layer in which selective dissolution of chromium occurred. The steady decline in the Ni:Cr ratio as

the maximal examined depth was approached was comparable to those observed in the base metal of the sterile control, indicating that the base metal of the nonsterile coupon may have been detected at the deepest assessed intervals. These results should, however, be considered in light of the inherent margin of error of XPS analysis (+/- 0.5 atomic %); therefore the differences that were observed may not be significant.

When XPS analysis of several different surface areas of sterile- and nonsterile-incubated coupons was performed, no nickel or chromium was detected on the Alloy 22 surface incubated with YM bacteria, while both nickel and chromium were evident on some examined areas of the sterile-incubated coupon (Table 4). Coincident with the presence of nickel and chrome on sterile surfaces, oxygen content was also greater (Table 4); therefore the chrome and nickel that was detected might be areas of passive film metal oxides exposed between areas of media precipitates on the surface of this sterile-incubated coupon. Supporting this supposition is the finding that oxygen levels on nonsterile surfaces are significantly less than those on sterile surfaces, and these lower values are on par with those observed using the XPS depth analysis of the biofilm (data not shown). Given that no Alloy 22 components were evident on the surface of the biofilm present on the nonsterile coupon does not exclude the possibility that there may be metal precipitates (in fact a chromium precipitate was detected using SEM/EDS, above) present in other locales or within the biofilm, but none were detectable in this particular analysis. Non-detection of nickel, molybdenum, or chromium precipitates on the nonsterile coupon is consistent with a selective mode of Alloy 22 dissolution whereby the solubilized Alloy 22 elements stay in solution rather than a homogeneous dissolution of all elements with subsequent precipitation of selective components (Fig. 2).

Table 4. XPS Elemental Analysis of Surface Sites on Alloy 22

	Nonsterile Surface (atomic% [a])				Sterile Surface (atomic% [a])			
Element	**Spot 1[b]**	**Spot 2[b]**	**Spot 3[b]**	**Spot 4[c]**	**Spot 1[b]**	**Spot 2[b]**	**Spot 3[b]**	**Spot 4[c]**
Ni	n.d.[d]	n.d.	n.d.	n.d.	n.d.	n.d.	0.1	0.2
Cr	n.d.	n.d.	n.d.	n.d.	n.d.	0.3	1.2	0.9
C	94.8	95.5	95.8	95.6	81.7	83.6	72.2	78.7
O	3.8	3.3	3.0	3.2	13.7	12.2	19.6	14.8
Si	1.4	1.2	1.2	0.8	3.9	3.9	3.4	3.7

[a] +/– 0.5 atomic %
[b] 1 mm diameter
[c] 3×10 mm^2
[d] not detected

Silicon was detected on both the nonsterile and the sterile Alloy 22 surface; silica precipitates had to originate from the 100X J13 well water solvent, which was the only source of silicon present. It is interesting to note, however, that significantly more silica was evident on the sterile surface, suggesting that the biofilm present on the biotic coupon may be masking siliceous precipitates, just as it may be occluding detection of metal precipitates.

CONCLUSIONS

Prior studies had suggested that YM bacteria might be responsible for potential selective dissolution of specific alloying elements from Alloy 22. The alternative scenario of metal dissolution is that all metal elements homogeneously solubilize at the same rates such that the remaining metal composition is stoichiometrically equivalent to unaffected base metal. Stoichiometric dissolution infers that the amount of an alloying element that solubilizes is in direct proportion to its occurrence in base metal. Because evaluation of solubilized metal components (and recovered precipitates) was not satisfactory to conclusively discern between selective or stoichiometric dissolution of Alloy 22, XPS interrogation of the surface of treated and control coupons was undertaken. The results were inconclusive due to the excessive roughness of the surface of analyzed coupons, resulting in a loss of resolution in the detection of specific layers; a potential dealloyed layer under these conditions was therefore difficult to identify. However, the results do show that this high resolution analysis of the surface with XPS is a feasible technique to determine dissolution modes. Possible occurrence of selective dissolution was detected as indicated by a potentially chromium depleted region of bacterially inoculated coupons. Also, lack of metal precipitates on the surface of these coupons points to selective dissolution as a mode of dissolution of Alloy 22 under the tested conditions. Presently, mirror finish coupons of Alloy 22 are being treated in similar tests to allow the potential identification of a dealloyed region below the protective oxide film of bacterially-inoculated coupons. Using a smooth surface on test coupons will increase the resolution of XPS results, to definitively determine the mode of Alloy 22 dissolution. Additionally, a greater number of like-treated samples needs to be assessed to increase the confidence of future findings

ACKNOWLEDGEMENTS

The authors gratefully acknowledge the expert technical services of Cheryl Evans, who performed XPS analysis. The authors also thank Christine Orme and Art Nelson for their help in evaluating the analytical approach and experimental results. This work was performed under the auspices of the U.S. Department of Energy by the University of California, Lawrence Livermore National Laboratory under Contract No. W-7405-Eng-48, and was supported by the Yucca Mountain Site Characterization Project.

REFERENCES

1. D.S. Dunn, C.S. Brossia, O. Pensado, "Long-Term Dissolution Behavior of Alloy 22: Experiments and Modeling," Corrosion/2001, Paper no. 01125, (Houston TX:NACE Intl, 2001).
2. Office of Civilian Radioactive Waste Management (OCRWM), "General Corrosion and Localized Corrosion of Waste Package Outer Barrier," ANL-EBS-MD-000003, Rev. 00, January 2000.
3. S. Boudin, J-L. Vignes, G. Lorang, M. Da Cunha Belo, G. Blondiaux, S.M. Mikhailov, J.P. Jacobs, H.H. Brongersma, Surface and Interface Analysis 22(1994): p. 462-466.
4. D.D. McDonald, J. Electrochem. Soc., 139(1992): p. 3434-3439.
5. T. Lian, S. Martin, D. Jones, A. Rivera, J. Horn, "Corrosion of Candidate Container Materials by Yucca Mountain Bacteria," Corrosion/1999, Paper no. 476, (San Antonio TX: Nace Intl, 1999).
6. D.J. Reasoner and E.E. Geldreich, Appl. Environ. Microbiol. 49(1985): p.1.
7. J.M. Delaney, "Reaction of Topopah Spring Tuff with Water: A Geochemical Modeling Approach Using the WEQ3/6 Reaction Path Code," Lawrence Livermore Natl. Laboratory, Report UCID-53631, November, 1985.